Effect of Silicon-on-Insulator Substrate on Residual Strain in 3C-SiC Films *

Wang Xiaofeng[1], Huang Fengyi[1], Sun Guosheng[1], Wang Lei[1], Zhao Wanshun[1], Zeng Yiping[1], Li Haiou[2], and Duan Xiaofeng[2]

(1 *Institute of Semiconductors, Chinese Academy Sciences, Beijing* 100083, *China*)
(2 *Institute of Physics, Chinese Academy of Sciences, Beijing* 100080, *China*)

Abstract: One group of SiC films are grown on silicon-on-insulator (SOI) substrates with a series of silicon-over-layer thickness. Raman scattering spectroscopy measurement clearly indicates that a systematic trend of residual stress reduction as the silicon over-layer thickness decreases for the SOI substrates. Strain relaxation in the SiC epi-layer is explained by force balance approach and near coincidence lattice model.

Key words: Raman; strain relaxation; force balance principle; near coincidence lattice model
PACC: 3220F; 6855
CLC number: TN304.2+4 **Document code:** A **Article ID:** 0253-4177(2005)09-1681-07

1 Introduction

Due to its special properties related to the wide bandgap, SiC is among the best candidates for high-power, high-temperature, and high-frequency electronics applications. One of the potential approaches for the growth of epitaxial 3C-SiC is to use silicon as substrate, taking advantage of its low cost and compatibility with the modern CMOS technology. However, the large lattice mismatch and thermal mismatch constitute major obstacles for the growth of high quality heteroepitaxial 3C-SiC films with less strain on Si substrate.

Silicon on insulator (SOI) substrate has been proposed as a promising complicate substrate for 3C-SiC deposition[1]. The basic idea is to grow SiC on thin-film Si, physically isolated from the bulk Si substrate by buried oxide (BOX)[1~2]. It is expected that the misfit strain can therefore be transferred from the top epitaxial layer to the underneath silicon-over-layer (SOL) thin film according to the principle of strain partitioning[3]. The thinner the SOL layer is, the less the top epitaxial layer will be strained. Experimental observation of strain reduction in SiC on SOI has been a controversial topic[4], with convincing results reviewed in recent publications[1,5]. The ideal situation is that the whole SOL layer be converted into SiC during the carbonization process. Until now, few reports have been published about such case where the SOL layer and BOX layer were consumed completely after carbonization. Whether this kind of SiC/Si (because the SOL and the BOX layer have disappeared, the samples have a SiC/Si structure) is the same as SiC grown on Si substrate or not has yet to be researched.

In this paper, we investigate the special situation. One group of SOI substrates with a series of silicon-over-layer thickness were used to grow SiC.

* Project supported by the National High Technology Research and Development Program of China (No. 2002AA311220)
Wang Xiaofeng female, PhD candidate. Her major research interest is in growth of SiC films on SOI and fabrication of SiC devices. Email: xiaofw@red.semi.ac.cn
Received 28 February 2005, revised manuscript received 24 May 2005

The disappearance of the SOL and BOX layers was achieved by an extra high temperature heat after the normal carbonization process. Si substrate was used for comparison. The residual strain in the SiC films was measured by Raman scattering spectroscopy. Force balance approach and near coincidence lattice model were used to explain the strain relaxation in the large lattice mismatch system of SiC and Si.

2 Experiment

Commercial on-axis (001) Si and (001) SOI wafers were used for the SiC growth. The SOI substrates had 140nm/800nm SOL/BOX. A thinner compliant substrate was expected to achieve more strain transfer from the epilayer[6]. Different SOL thicknesses were achieved by chemical etching ($HF : HNO_3 = 1 : 1$). SOI wafers with 36nm and 13.5nm SOL were obtained. SiC grown on Si substrates had also been prepared for comparison.

Heteroepitaxial growth was performed in a homemade horizontal low-pressure chemical vapor deposition (LPCVD)[7] reactor at a pressure of 2.6×10^4 Pa using SiH_4 and C_2H_4 as the precursors. To ensure comparative studies, samples from the same group were placed side by side in the growth chamber, and substrate holder was rotating during the growth.

The growth conditions were as follows: the Si surfaces were pre-carbonized by heating the substrates from room temperature to 1100 ℃ for 3min. After carbonization, the substrates were heated at 1220 ℃ for another 3min under H_2 flow of 3L/min. The growth temperature, C/Si ratio, and hydrogen flow were 1200 ℃, 4, and 3L/min, respectively. The growth period was 1h and the sample thicknesses were approximately 1.1μm.

The epilayers were characterized using X-ray diffraction (XRD), AFM, TEM, and Raman measurements. XRD measurements were performed with a single-crystal X-ray diffractometer (Rigaku-2400). The surface morphology of the sample surfaces after carbonization was analyzed by using a NanoScope IIIa-D3000 AFM with contact mode. A Philips CM200 super-twin field emission gun (FEG) TEM was also employed to observe microstructures of the SiC films with point-to-point resolution of approximately 0.24nm. High resolution TEM (HRTEM) examination was performed on JEM-2010. Raman measurements were performed with a multichannel modular triple Raman system (JY-T64000) with confocal microscopy. A solid-state diode laser at 488nm (Verdi-2 from Coherent Company) was used as an excited source. The output power of the argon ion laser was maintained at 100mW and focused onto the samples through an Olympus microscope with a 100X objective lens. The spot diameter of the focused laser beam on the sample was approximately 1μm. All measurements were taken at room temperature. The JY-T64000 was calibrated using a Hg lamp and a 〈100〉 silicon reference sample. The resolution of the instrument was approximately 1.8cm^{-1}, but the peak position could be fitted to within ±0.2cm^{-1}.

3 Results and discussion

Figure 1 shows the XRD spectrum for the 3C-SiC film on SOI with SOL thickness of 36nm. Three peaks corresponding to Si (200), SiC (200), and Si (400) are observed. Broad features are observed at the bottom of the Si (200) peak and the Si (400) peak. This might be related to the lattice disorder in the strained SOI substrate taking into account the thinned SOL layer. No other peaks are observed.

HRTEM was used to analyze the structure of the interface which is more complicated because of lattice mismatch. Figure 2 shows the bright-field (BF) TEM image and the HRTEM image of the 3C-SiC films grown on SOI substrates for the same SiC sample used in Fig. 1. Other samples have the similar BF-TEM and HRTEM images. It is interesting to find in Fig. 2(a) that the buried SiO_2 layer disappeared, and the interface between SiC and Si

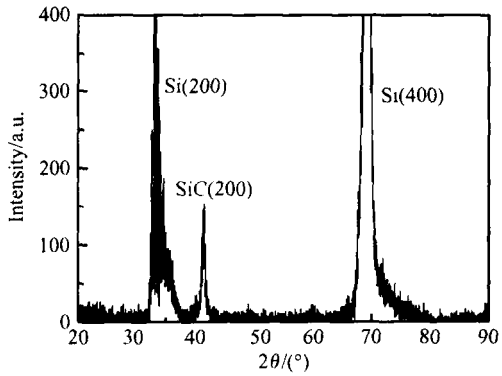

Fig. 1 XRD spectrum of 3C-SiC/ SOI film on SOI with SOL thickness of 36nm

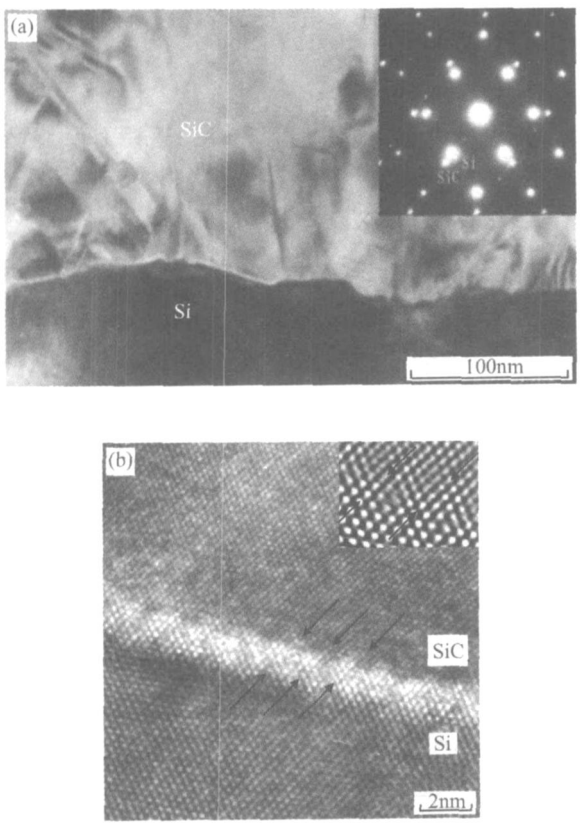

Fig. 2 Bright-field (BF) TEM image (a) and HRTEM image (b) of 3C-SiC film on SOI with SOL thickness of 36nm The inset in (a) is the corresponding selected area electron diffraction (SAED) pattern from the interface region. In the right top of (b) is the Fourier transform (FT) of HRTEM image.

was wavy. No cavity can be found near the interface. These will be explained later. Micro-twins and stacking faults (SFs) can be seen in the SiC epilayer clearly. To evaluate the density of the micro-twins and stacking faults, the corresponding selected area electron diffraction (SAED) pattern from the interface region is observed and shown in the inset of Fig. 2(a). The well alignment of the SiC diffraction spots with the Si spots indicates that the epitaxial relationship between the SiC film and the Si substrate is almost perfect. The weak twin spots corresponding to the faults and defects observed in Fig. 2(a) demonstrate that the density of the microtwins and stacking faults is rather low.

The HRTEM image in Fig. 2(b) shows the lattice fringes of Si and SiC across the interface. The zig-zag chains are observed between the interface of SiC and Si. The array of periodic strain contrast along the interface is marked with arrows. The Fourier transform (FT) of HRTEM image in the right top shows that the spacing of the regions with perfect lattice matching corresponds to the 5 ∶4-ratio of their lattice constants.

The disappearance of the SOL and the BOX might be induced by the extra heat after the carbonization process, because we did not find similar phenomena in the case of the normal carbonization and growth experiments. The SiC carbonization layer was formed by the silicon out-diffusion[8] and carbon in-diffusion[9]. At least 20 % of the surface is uncovered by SiC buffer layer when the SOL thickness is less than 150nm, and nearly 50 % is uncovered when less than 50nm[8]. And the uncovered BOX was exposed to the H_2 ambient. Therefore, the extra heating process can be regarded as an in-situ H etching[10]. The oxide was removed in the form of SiO gas[10~12]. The residual SOL which might be remaining after the carbonization process can be decomposed according to the reaction[8,13~15]:

$$Si + SiO_2 \Rightarrow SiO$$

In addition, the carbon-containing gas contributed to the consumption of the SiO_2 through the interaction of the Si - O - C bonds[16]. Finally, SiC fragments collapse on the Si substrate along with the consumption of the SOL and the BOX. The wavy interface in Fig. 2(a) indicates that except for the

decomposition of the BOX, the Si substrate underneath the SOL and BOX layers had been exhausted to a degree.

Figure 3(a) shows the Raman spectra for the four samples. The plots have been offset for clarity. Curve *a* corresponds to SiC film on Si substrate, and curves *b*, *c*, and *d* correspond to SiC films on SOI with SOL thickness of 100, 36, and 13.5nm, respectively. By fitting the TO lines with the Lorentzian fit function, we get the TO peaks at 790.9, 790.8, 791.1, and 792.0cm^{-1} for curves *a*, *b*, *c*, and *d*, respectively. There is no obvious peak shifts for curves *a* and *b* considering the repeatability error of $\pm$0.2cm^{-1}. The LO lines of SiC locate at $\sim$796cm^{-1}. The broad peak corresponds to the second optical Raman phonon of Si.

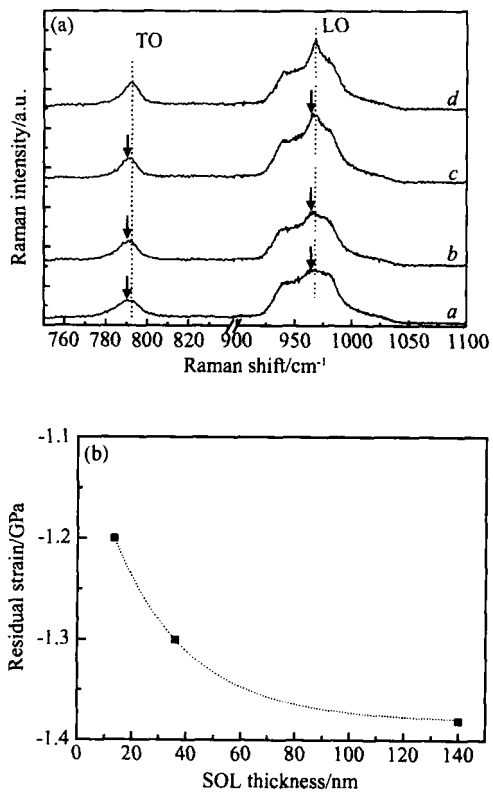

Fig. 3 (a) Raman spectra for the SiC films The plots have been offset for clarity. Curve *a* corresponds to SiC film on Si substrate. Curves *b*, *c*, and *d* correspond to SiC films on SOI with SOL thickness of 100, 36, and 13.5nm, respectively; (b) Dependence of residual strain in SiC films on SOL thickness

The dependence of residual strain in SiC films on SOL thickness is shown in Fig. 3(b). The residual strain was calculated according to the relationship of Raman shift with hydrostatic strain[17]. Peak position (796.2cm^{-1})[18] of free 3C-SiC film was taken as reference. A negative sign corresponds to tensile stress. The dotted line is an exponential fit to the data, in an effort to clearly observe the residual strain decrease in SiC film along with the thinning of the SOL thickness. This demonstrates that these kind of SiC/Si samples are not the same as SiC grown on Si substrate. The results can be explained by the force balance approach and the near coincidence lattice model.

The force balance principle is put forward to solve the strain partition between the substrate and the lattice-mismatched epitaxial layer[19~21]. The elastic strain in the epilayer can be calculated by

$$\sigma_f = \Delta \frac{h_s k_s}{h_s k_s + h_f k_f} k_f \qquad (1)$$

where Δ is the lattice mismatch percentage, h_s is the thickness of the substrate, h_f is the thickness of the epilayer, k_s is the effective coefficient of the substrate, and k_f is the effective elastic coefficient of the epilayer. The lattice mismatch percentage is 20% for the SiC/Si system. The values of k_s and k_f are 7.48 and 144GPa for Si and 3C-SiC, respectively[22].

It should be mentioned that Equation (1) is valid only when the thickness of the epilayer is less than the critical thickness. Until now, none has reported the experimental or calculated critical thickness for the 3C-SiC/Si system. One reason is that the critical thickness for the large lattice mismatch system is so small that it is difficult to determine. And the presence of double-positioning boundaries (DPB's) and/or stacking faults (SF's), which complicates the definition of the Burgers vector, is another reason.

Here we estimate the critical thickness according to the surface morphology. For film thicknesses above the critical thickness, growth is in the form of 3D columnar islands. The edges of these islands

are possible surfaces for dislocation termination[23]. The AFM image for the SiC film on SOI with 36nm SOL after carbonization is shown in Fig. 4. Many big and small island-shaped SiC bumps are observed, indicating the occurrence of Stranski and Krastanov (SK) growth mode[8]. The big SiC bumps have thickness of about 10nm. The RMs roughness for an area of 2μm ×2μm is found to be 5.68nm, which is much bigger than a single Si-C bilayer. Therefore, the SiC thickness after carbonization is above the critical thickness. Here we assume the critical thickness is the carbonization thickness (~10nm)[8], although the calculated data may be a little lower.

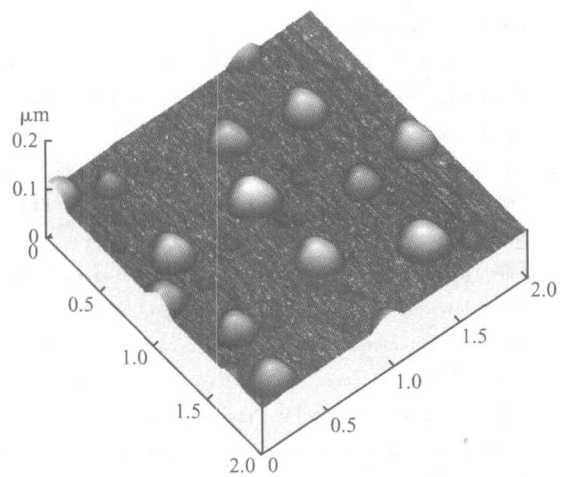

Fig. 4 AFM image for the SiC film on SOI with 36nm SOL after carbonization

The residual elastic strain in the SiC layer deduced from Eq. (1) is 9.85, 4.54, and 1.89 GPa for SiC on SOI with SOL thickness of 140, 36, and 13.5nm, respectively. The data are shown in Fig. 5 and marked with open circles. The data in Fig. 3(b) are also shown here for comparison and marked with filled squares. The two groups of data become closer when the SOL thickness decreases. The two curves cross at SOL thickness of ~10nm or below. This demonstrates that strain relaxation only dominate when the SOL thickness is low enough. The open-circle data is about 10 times of the filled squared data at SOL of 140nm. However, the largest residual strain difference is only 0.2 GPa for the set of filled square data. Other strain relaxation mechanisms should exist except the force balance principle. We attribute it to the near coincidence lattice model[24].

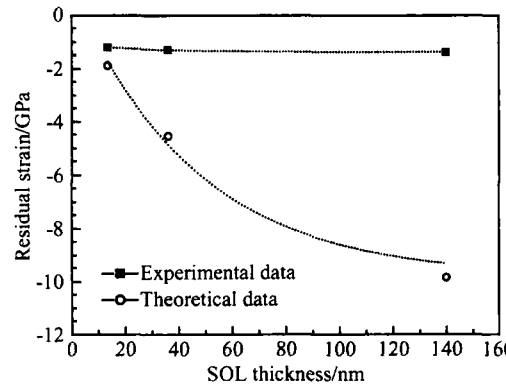

Fig. 5 Dependence of residual strain in SiC on SOL thickness with the theoretical data marked with open circle and the experimental data marked with filled square The set of the filled square data is the same as those shown in Fig. 3(b), and is plotted here for comparison.

Near perfect coincidence lattice with a lattice plane ratio of 5/4 can be observed in the Fourier transform (FT) of HRTEM image in Fig. 2(b). The edge type dislocations are observed. This kind of misfit dislocations is generated at the interface during the formation of the 3D critical nuclei. The large lattice misfit strain is relieved by the regularly arranged misfit dislocations. The actual lattice mismatch will be reduced to about 0.4%, a reasonable value to guarantee the stabilization of epitaxial growth. The deviation from perfect coincidence is of great importance because it defines the amount of residual strain in the epilayer. Therefore, the explaining why the actual residual strain in SiC differs little is conducted. The large lattice mismatch is accommodated mainly through the coincidence lattice model when the substrate thickness is above the critical thickness. In our experiment, the SOI substrate with 140nm SOL does not play the role of compliant substrate compared with the case of Si substrate. And then the similarity of curves *a* and *b* in Fig. 3(a) is understandable.

In our analysis, thermal strain was omitted.

The thermal strain is less than 0.15 GPa for our growth temperatures[25].

4 Conclusion

Heteroepitaxial SiC films were grown on SOI with different SOL thickness. The disappearance of the SOL and the BOX was observed by HRTEM as the result of an extra high temperature heating after the carbonization process. Measurement of Raman scattering spectroscopy clearly indicates a systematic trend of residual stress reduction as the silicon over-layer thickness decreases for the SOI substrates. This demonstrates that strain transfer from the epilayer to the underneath SOL occurs during carbonization process. The large lattice mismatch is accommodated mainly through the coincidence lattice model when the substrate thickness is above the critical thickness.

Acknowledgement The authors would like to express their thanks to Y. R. Liu at the Institute of Physics, Chinese Academy of Sciences for his help in Raman measurements.

References

[1] Camassel J. State of the art of 3C-SiC/silicon on insulators. J Vac Sci Technol B, 1998, 16(3): 1648

[2] Metzger R A. SOI without SOI substrates. Compound Semiconductor Magazine, 2000, 6(7): 1

[3] Lo Y H. New approach to grow pseudomorphic structures over the critical thickness. Appl Phys Lett, 1991, 59(18): 2311

[4] Lee B T, Moon C K, Song H J, et al. Chemical-vapor-deposition growth and characterization of epitaxial 3C-SiC films on SOI substrates with thin silicon top layers. J Mater Res, 2001, 16(1): 24

[5] Park J H, Kim J H, Kim Y, et al. Effects of silicon-on-insulator substrate on the residual stress within 3C-SiC/Si thin films. Appl Phys Lett, 2003, 83(10): 1989

[6] Chua C L, Hsu W Y, Lin C H, et al. Overcoming the pseudomorphic critical thickness limit using compliant substrates. Appl Phys Lett, 1994, 64(26): 3640

[7] Sun Guosheng, Wang Lei, Luo Muchang, et al. Improved epitaxy of 3C-SiC layers on Si(100) by new CVD/LPCVD system. Chinese Journal of Semiconductors, 2002, 23(8): 800

[8] Papaioannou V, Moller H, Rapp M, et al. Evolution of cavities in Si at the 3C-SiC/Si interface during 3C-SiC deposition by LPCVD. Mater Sci Eng B, 1999, 61/62: 539

[9] Bustarret E, Vobornik D, Roulot A, et al. Interfacial strain in 3C-SiC/Si(100) pseudo-substrates for cubic nitride epitaxy. Phys Status Solidi A, 2003, 195(1): 18

[10] Young J D, Du Jiangang, Zorman A C, et al. High-temperature single-crystal 3C-SiC capacitive pressure sensor. IEEE Sensors Journal, 2004, 4(4): 464

[11] Gerro G, Planes N, Papaioannou V, et al. Spectroscopic ellipsometry studies of heteroepitaxially grown cubic silicon carbide layers on silicon. Mater Sci Eng B, 1999, 61/62: 586

[12] Möller H, Krötz G, Eickhoff M, et al. Suppression of Si cavities at the SiC/Si interface during epitaxial growth of 3C-SiC on silicon-on-insulator. J Electrochem Soc, 2001, 148(1): G16

[13] Gerro G, Planes N, Papaioannou V, et al. Role of SIMOX defects on the structural properties of -SiC/SIMOX. Mater Sci Eng B, 1999, 61/62: 586

[14] Papaioannou V, Pavlidou E, Stoemenos J, et al. Structural characterization of 3C-SiC epitaxially grown on Si-on-insulator. Mater Sci Forum, 1998, 264～268: 445

[15] Smith F W, Ghidim G. Reaction of oxygen with Si (111) and (100): critical conditions for the growth of SiO_2. J Electrochem Soc, 1982, 129: 1300

[16] Lucovsky G, Niimi H S. Remote plasma-assisted oxidation of SiC: a low temperature process for SiC-SiO_2 interface formation that eliminates interfacial Si oxycarbide transition regions. J Phys Condensed Matter, 2004, 16(17): S1815

[17] Diego O, Cardona M, Vogl P. Pressure dependence of the optical phonons and transverse effective charge in 3C-SiC. Phys Rev B, 1982, 25: 3878

[18] Feldman D W, Parker J H, Choyke W J, et al. Phonon dispersion curves by raman scattering in SiC, polytypes 3C, 4H, 6H, 15R, and 21R. Phys Rev, 1968, 173: 787

[19] Zhang Zhicheng, Yang Shaoyan, Chen Yonghai, et al. Compliant substrate technology in the strain hetero-epitaxy. Research in Metallic Material, 2002, 28(2): 1 (in Chinese) [张志成, 杨少延, 陈涌海, 等. 应变异质外延中的柔性衬底技术. 金属材料研究, 2002, 28(2): 1]

[20] Wang Xiaofeng, Wang Lei, Zhao Wanshun, et al. 3C-SiC growth on SOI with high silicon-over-layer. Chinese Journal of Semiconductors, 2004, 25(12): 1652 (in Chinese) [王晓峰, 王雷, 赵万顺, 等. 厚表层 Si 柔性绝缘衬底上 SiC 薄膜的外延生长. 半导体学报, 2004, 25(12): 1652]

[21] Carter-Coman C, Brown A S, Bicknell-Tassius R, et al. Strain-modulated epitaxy: a flexible approach to 3-D band structure engineering without surface patterning. Appl Phys Lett, 1996, 69(2): 257

[22] Mukaida H, Okumura H, Lee J H, et al. Raman scattering of SiC: Estimation of the internal stress in 3C-SiC on Si. J Appl Phys, 1987, 62: 254

[23] Mahajan S. Large lattice mismatch epitaxy. Materials Research Society Symposium-Proceedings, Covalent Ceramics Ⅲ-Science and Technology of Non-Oxides, 1996, 410: 3
[24] Fletcher N H, Lodge K W. Energy of interfaces between crystals: an *ab initio* approach. SAE Preprints, 1975, Pt B: 529
[25] Feng Z C, Choyke W J, Powell J A. Raman determination of layer stresses and strains for heterostructures and its application to the cubic SiC/Si system. J Appl Phys, 1988, 64: 6827

SOI 衬底对 3C-SiC 异质外延薄膜内残存应力的影响*

王晓峰[1]　黄风义[1]　孙国胜[1]　王　雷[1]　赵万顺[1]
曾一平[1]　李海鸥[2]　段晓峰[2]

(1 中国科学院半导体研究所, 北京　100083)
(2 中国科学院物理研究所, 北京　100080)

摘要: 在一组具有不同厚度表层硅的 SOI 衬底上异质外延 SiC 薄膜. Raman 测试结果表明, SiC 薄膜中的残存应力随着表层硅厚度的减薄而降低. 采用力平衡原理和重合位置点阵模型对 SiC 外延层中的应力释放现象进行了解释.

关键词: 喇曼; 应力释放; 力平衡原理; 重合位置点阵模型
PACC: 3220F; 6855
中图分类号: TN304. 2+4　　**文献标识码**: A　　**文章编号**: 0253-4177(2005)09-01681-07

*国家高技术研究发展计划资助项目(批准号:2002AA311220)
王晓峰　女, 博士研究生, 主要从事 SOI 衬底上 SiC 薄膜的生长及其器件的研究. Email: xiaofw@red.semi.ac.cn
2005-02-28 收到, 2005-05-24 定稿